

# Time Course and $\text{Ca}^{2+}$ Dependence of Sensitivity Modulation in Cyclic GMP-gated Currents of Intact Cone Photoreceptors

TATIANA I. REBRIK, EKATERINA A. KOTELNIKOVA, and JUAN I. KORENBROT

From the Department of Physiology, School of Medicine, University of California at San Francisco, San Francisco, California 94143

**ABSTRACT** We determined the  $\text{Ca}^{2+}$  dependence and time course of the modulation of ligand sensitivity in cGMP-gated currents of intact cone photoreceptors. In electro-permeabilized single cones isolated from striped bass, we measured outer segment current amplitude as a function of cGMP or 8Br-cGMP concentrations in the presence of various  $\text{Ca}^{2+}$  levels. The dependence of current amplitude on nucleotide concentration is well described by the Hill function with values of  $K_{1/2}$ , the ligand concentration that half-saturates current, that, in turn, depend on  $\text{Ca}^{2+}$ .  $K_{1/2}$  increases as  $\text{Ca}^{2+}$  rises, and this dependence is well described by a modified Michaelis-Menten function, indicating that modulation arises from the interaction of  $\text{Ca}^{2+}$  with a single site without apparent cooperativity.  $^{\text{Ca}}K_m$ , the Michaelis-Menten constant for  $\text{Ca}^{2+}$  concentration is  $857 \pm 68$  nM for cGMP and  $863 \pm 51$  for 8Br-cGMP. In single cones under whole-cell voltage clamp, we simultaneously measured changes in membrane current and outer segment free  $\text{Ca}^{2+}$  caused by sudden  $\text{Ca}^{2+}$  sequestration attained by uncaging diazo-2. In the presence of constant 8Br-cGMP,  $15 \mu\text{M}$ ,  $\text{Ca}^{2+}$  concentration decrease was complete within 50 ms and membrane conductance was enhanced  $2.33 \pm 0.95$ -fold with a mean time to peak of  $1.25 \pm 0.23$  s. We developed a model that assumes channel modulation is a pseudo-first-order process kinetically limited by free  $\text{Ca}^{2+}$ . Based on the experimentally measured changes in  $\text{Ca}^{2+}$  concentration, model simulations match experimental data well by assigning the pseudo-first-order time constant a mean value of  $0.40 \pm 0.14$  s. Thus,  $\text{Ca}^{2+}$ -dependent ligand modulation occurs over the concentration range of the normal, dark-adapted cone. Its time course suggests that its functional effects are important in the recovery of the cone photoreponse to a flash of light and during the response to steps of light, when cones adapt.

**KEY WORDS:** retina • ligand-gated ion channel • phototransduction • adaptation • teleost fish

## INTRODUCTION

Rods and cone photoreceptors in the vertebrate retina continuously adjust the gain and kinetics of their photoreponse as a function of background light intensity. These adjustments, known as adaptation, allow photoreceptors to respond to signals that differ little in intensity from the background light, regardless of the absolute intensity of that background. The extent of adaptation reflects the relative contribution of three distinct cellular mechanisms. (a) Response compression, which arises from the nonlinear relation between response amplitude and light intensity. (b) Neural adaptation, which arises from modulation of the biochemical cascade that underlies phototransduction. (c) Pigment adaptation, which arises from biochemical events associated with photopigment bleaching (reviewed in Fain et al., 1996; Perlman and Normann, 1998). At light levels that do not cause significant pigment bleaching, response-compression dominates the mechanisms of light adaptation in mammalian rods, including humans,

and, therefore, rods exhibit response saturation (reviewed in Pugh and Lamb, 1990; Perlman and Normann 1998). Rods in lower vertebrates exhibit some neural adaptation, but even in these species limiting background intensity exists at which rods, but not cones, become unresponsive (Fain, 1976; Kleinschmidt and Dowling, 1975; Miller and Korenbrot, 1993). Cones, in contrast, are characterized by more powerful means to modulate the phototransduction process and, therefore, they do not exhibit response saturation even when background illumination is raised by 6–7 log units (Normann and Werblin, 1974; Normann and Perlman, 1979; Malchow and Yazulla, 1986; Burkhardt, 1994).

In isolated, dark-adapted photoreceptors, adaptation begins to be discerned by the time the peak of the photoreponse is reached, and it then smoothly reaches a stationary state within a second or two (reviewed in Fain and Matthews, 1990; Pugh and Lamb, 1990). In the intact eyecup, however, photoreceptor adaptation appears to occur in several steps. The first step is similar to that characterized in isolated cells. Additional, slower ones allow continuing improvement of the cone's sensitivity to light and a stationary condition is attained only after 2–3 min of continuous illumination (Normann and Perlman, 1979; Burkhardt, 1994).

Address correspondence to Juan I. Korenbrot, Dept. of Physiology, School of Medicine, Box 0444, University of California at San Francisco, San Francisco, CA 94143. Fax: 415-476-4929; E-mail: juan@itsa.ucsf.edu

In rods and cones, light-dependent changes in outer segment cytoplasmic  $\text{Ca}^{2+}$  must occur for neural adaptation to proceed. If these changes are prevented, dark-adapted photoreceptors respond to light, but the photoresponses are altered in their light sensitivity, time course, and adaptation features (reviewed in Fain and Matthews, 1990; Pugh and Lamb, 1990). The mechanisms of action of  $\text{Ca}^{2+}$  are not understood in detail, but  $\text{Ca}^{2+}$  modulates the activity of several steps in the phototransduction cascade. In rods,  $\text{Ca}^{2+}$  modulates: (a) ATP-dependent deactivation (Lagnado and Baylor, 1994; Sagoo and Lagnado, 1997); (b) rhodopsin phosphorylation, through the action of recoverin (S-modulin) (Kawamura, 1993; Chen et al., 1995); (c) catalytic activity of guanylyl cyclase (Lolley and Racz, 1982; Pepe et al., 1986; Koch and Stryer, 1988), through the action of GCAP proteins (Palczewski et al., 1994; Dizhoor et al., 1995); (d) cGMP sensitivity of the cyclic nucleotide-gated ion channels (CNG channels),<sup>1</sup> through the action of a factor similar to, if not the same as, calmodulin (Hsu and Molday, 1994; Bauer, 1996). Much less is known about the mechanisms of action of  $\text{Ca}^{2+}$  on the transduction cascade in cones. Indirect studies indicate that  $\text{Ca}^{2+}$  regulation of guanylyl cyclase in cones can be similar to that in rods (Miller and Korenbrot, 1994) and the cloning of a cone-specific S-modulin (Kawamura et al., 1996) suggests that  $\text{Ca}^{2+}$ -dependent modulation of cone-opsin phosphorylation is a likely event. In cones, too, the nucleotide sensitivity of the CNG channels is modulated by  $\text{Ca}^{2+}$  (Rebrik and Korenbrot, 1998) through the action of a factor that is not calmodulin (Hackos and Korenbrot, 1997; Haynes and Stotz, 1997). To understand the specific role of these biochemical events in the process of adaptation, it is necessary to know in detail their dependence on  $\text{Ca}^{2+}$  and their time course.

In rods, every one of the events described above has been shown to depend on  $\text{Ca}^{2+}$  at concentrations that overlap those expected in dark- and light-adapted cells, somewhere between 10 and 1,000 nM. The time course of each of the various possible  $\text{Ca}^{2+}$  biochemical actions is poorly understood and the relationship between these dynamics and the time course of adaptation is largely undefined (Koutalos et al., 1995; Murnick and Lamb, 1996; Matthews, 1997). In rod outer segment homogenates, guanylyl cyclase and rhodopsin kinase activity respond to abrupt  $\text{Ca}^{2+}$  changes with a time constant that has upper limit of  $\sim 1$  s (Calvert et al., 1998).

$\text{Ca}^{2+}$  modulates the ligand sensitivity of CNG channels. The value of  $K_{1/2}$ , the concentration necessary to activate half-maximal current, increases as  $\text{Ca}^{2+}$  rises. In membrane patches detached from outer segments

of either rods or cones,  $K_{1/2}$  changes  $\sim 1.5$ -fold between its extreme values (Gordon et al., 1995; Hackos and Korenbrot, 1997). In intact rod outer segments, the total  $\text{Ca}^{2+}$ -dependent change in  $K_{1/2}$  is also  $\sim 1.5$  (Nakatani et al., 1995; Sagoo and Lagnado, 1996; Rebrik and Korenbrot, 1998). In intact cone outer segments, in contrast, the total magnitude of the shift is approximately fourfold (Rebrik and Korenbrot, 1998). Also, at a fixed cGMP concentration, the  $\text{Ca}^{2+}$  dependence of the cGMP sensitivity in rods has a midpoint at  $\sim 50$  nM, but the midpoint is  $\sim 290$  nM in cones. Because in rods the extent of change in  $K_{1/2}$  is small and occurs at  $\text{Ca}^{2+}$  concentrations expected only under bright illumination,  $\text{Ca}^{2+}$ -dependent channel modulation is expected to play a limited role in the control of gain and kinetics of the transduction signal. The converse arguments suggest that  $\text{Ca}^{2+}$ -dependent channel modulation may be of significant physiological consequence in cones.

To better understand the properties of CNG channel modulation in cones, we report here on an analysis of the  $\text{Ca}^{2+}$  dependence of  $K_{1/2}$  in electroporabilized cones (ep-cones), a preparation in which the cytoplasmic content of a single, intact outer segment can be rapidly controlled while measuring currents through the cGMP-gated channels. We also analyze the kinetics of this modulation in intact cones in which sudden changes in  $\text{Ca}^{2+}$  concentration are achieved with the use of a "caged"  $\text{Ca}^{2+}$  buffer, diazo-2 (Adams et al., 1989). In darkness, this compound binds  $\text{Ca}^{2+}$  with relatively low affinity because the buffer molecule, BAPTA, is linked by a photo-labile ester to a protecting group ("cage"). Upon absorption of ultraviolet light, the ester is cleaved and BAPTA is freed and able to sequester available free  $\text{Ca}^{2+}$ .

## MATERIALS AND METHODS

### Materials

Striped bass (*Morone saxatilis*) were obtained from Professional Aquaculture Services and maintained in the laboratory for up to 6 wk under 10:14-h dark:light cycles. The UCSF Committee on Animal Research approved protocols for the upkeep and killing of the animals. Diazo-2 and bis-fura-2 were purchased from Molecular Probes. Enzymes for tissue dissociation were obtained from Worthington Biochemicals. Zaprinast was from CalBiochem, all other chemicals were from Sigma-Aldrich.

### Photoreceptor Isolation

Under infrared illumination and with the aid of a TV camera and monitor, retinas were isolated from the eyes of fish dark adapted for 30–45 min. Single cones were isolated by mechanical trituration of retinas briefly treated with collagenase and hyaluronidase as described in detail elsewhere (Miller and Korenbrot, 1993). A Ringers' solution was used to isolate photoreceptors, to transfer them into the electrophysiological recording chamber, and to maintain them during the course of the experiments. The Ringers' composition was (mM): 136 NaCl, 2.4 KCl, 5  $\text{NaHCO}_3$ , 1  $\text{NaH}_2\text{PO}_4$ , 1  $\text{MgCl}_2$ , 1  $\text{CaCl}_2$ , 1  $\times$  MEM amino acids and vitamins,

<sup>1</sup>Abbreviations used in this paper: CNG channels, cyclic nucleotide-gated ion channels; PDE, phosphodiesterase.

10 glucose, 0.1 mg/ml BSA, and 10 HEPES. pH was 7.5 and osmotic pressure was 310 mOsM.

In experiments with tight-seal electrodes, cones were first isolated in a modified Ringers' in which pyruvate isosmotically replaced glucose. Cells were transferred in this solution onto the electrophysiological chamber, the bottom of which was a glass coverslip derivatized with Concanavalin A (3 mg/ml) (Picones and Korenbrot, 1992). Cells settled and firmly attached to the glass, and after 10 min the solution was exchanged for normal, glucose-containing Ringers'.

### *Suction Electrodes and Electroporabilization*

We measured the outer segment currents from single cones using suction electrodes, as described previously (Miller and Korenbrot, 1993). Electrodes were produced from Corning 1752 capillary glass ( $1.5 \times 1.0$ -mm o.d.  $\times$  i.d.) and coated with bis-dimethyl-amino di-methyl-silane. Suction electrodes were filled with a solution identical to the normal Ringers', except that  $\text{Ca}^{2+}$  concentration was  $1 \mu\text{M}$  and MEM components were omitted. Isolated photoreceptors were maintained in a recording chamber held on the stage of an inverted microscope. Under IR illumination, and observing with the aid of TV camera and monitors, individual cone outer segments were drawn into the electrode by gentle suction until the electrode tip sealed against the surface of the wider inner segment. Membrane currents were recorded at 0 mV holding voltage with a patch-clamp amplifier (EPC-7; List Instruments). Analogue signals were low-pass filtered below 50 Hz with an eight-pole Bessel filter and digitized on line (100 Hz) with a computer-based data acquisition system (FastLab; Indec).

Because the seal between suction electrode and single cones is low in impedance (few molarohms), there is an unavoidable drift in the recorded current. To minimize uncertainties due to this drift, we used a track-and-hold circuit before data digitization. The data acquisition software controlled this circuit and zeroed the current immediately before the delivery of test solutions. Data were accepted for analysis only if the holding current before and after the application of test solution (an interval of 45–70 s) differed by less than approximately  $\pm 20$  pA (typically approximately  $\pm 5\%$  of the maximum cGMP-dependent current). In any given data set, the error in the value of  $K_{1/2}$  due to drift can be calculated to be no worse than 1%. This error is negligible when compared with the variance from cell to cell, which is the limiting source of error in our data.

The cytoplasmic content of the cone outer segment was controlled by electroporabilizing the inner segment membrane and continuously superfusing with the "ep-solution," composed of (mM): 140 cholineCl, 5 glucose, 0.4 Zaprinast, and 10 HEPES. pH was 7.5 and osmotic pressure 310 mOsM. The ep-solution contained 1 mM free  $\text{Mg}^{2+}$  and various amounts of free  $\text{Ca}^{2+}$ , cGMP, or 8Br-cGMP, according to the design of the experiment. The solutions of defined  $\text{Ca}^{2+}$  and  $\text{Mg}^{2+}$  concentration were prepared by mixing appropriate amounts of  $\text{CaCl}_2$ ,  $\text{MgCl}_2$ , and the buffering agents EGTA (2 mM) or HEDTA (2 mM), calculated according to the equilibrium constant listed in Martell and Smith (1974).

The cone electroporabilization method is described in detail elsewhere (Rebrik and Korenbrot, 1998). In brief, a single cone was first drawn into a suction electrode, and then two sharp tungsten microelectrodes, electrically insulated except at their tip ( $1 \mu\text{m}$ ) (A-M Systems) were positioned opposite each other and pressed against the surface of the inner segment. Single, brief (1–10 ms) voltage pulses 1–5 V in amplitude were applied between the metal electrodes. Successful electroporabilization was apparent by a sudden and subtle change in the visual appearance of the inner segment membrane. Ep-solutions flowed continuously from a  $100\text{-}\mu\text{m}$  diameter glass capillary connected

through a micromanifold to solution reservoirs maintained under positive pressure (DAD-12; Adams and List). The ep-solutions were selected with electronically controlled switch valves, and solution changes were complete in  $<100$  ms.

### *Membrane Currents in Intact, Single Cones*

We measured membrane currents under voltage clamp using tight-seal electrodes in the whole-cell mode. Electrodes were produced from aluminosilicate glass ( $1.5 \times 1.0$  mm o.d.  $\times$  i.d., No. 1724; Corning Glassworks). Single cones were firmly attached to the glass bottom of a recording chamber and maintained in darkness on the stage of an inverted microscope equipped with DIC. Under IR illumination, and observing with the aid of TV camera and monitors, electrodes were sealed onto the side of the inner segment. Currents were recorded with a patch-clamp amplifier (Axopatch 1D; Axon Instruments, Inc.). Analogue signals were low-pass filtered below 200 Hz with an eight-pole Bessel filter (Kronh-Hite) and digitized online at 1 kHz (FastLab).

The tight-seal electrode-filling solution was composed of (mM): 115  $\text{K}^+$  gluconate, 20  $\text{K}^+$  aspartate, 33 KCl, 1 diazo2, 0.1 bis-fura2, 1.04  $\text{MgCl}_2$  (to yield 1 mM free  $\text{Mg}^{2+}$ ), 0.258  $\text{CaCl}_2$  (to yield 600 nM free  $\text{Ca}^{2+}$ ), and 10 MOPS. pH was 7.25 and osmotic pressure was 305 mOsM. Free  $\text{Ca}^{2+}$  and  $\text{Mg}^{2+}$  were calculated using the equilibrium constants reported for dark diazo-2 (Adams et al., 1989) and bis-fura-2. The solution could also contain 8Br-cGMP and Zaprinast (0.4 mM), but it lacked triphosphate nucleotides and, therefore, could not sustain endogenous synthesis of cGMP (Hestrin and Korenbrot, 1987; Rispoli et al., 1993).

### *Uncaging Diazo-2 and Measuring the Rate of $\text{Ca}^{2+}$ Sequestration In Vivo*

The instrument we developed to uncage and simultaneously measure membrane current and fluorescence in isolated, dark-adapted bass single cones is described in detail elsewhere (Ohyama, T., D.H. Hackos, S. Frings, V. Hagen, U.B. Kaupp, and J.I. Korenbrot, manuscript submitted for publication).  $\text{Ca}^{2+}$  concentration was monitored using bis-fura-2, a structural analogue of fura-2 with slightly lower affinity for  $\text{Ca}^{2+}$  ( $K_d \sim 520$  nM in the presence of 1 mM  $\text{Mg}^{2+}$ ) and higher molar extinction coefficient than fura-2. Fluorescence was excited by 380-nm light and emission intensity measured in the range between 410 and 600 nm using a photomultiplier operated in photon counting mode (50-ms counting bins). Our instrument allowed us to use relatively low intensity 380-nm light to excite bis-fura-2 fluorescence ( $2.55 \times 10^8$  photons  $\cdot \mu\text{m}^{-2} \text{s}^{-1}$ ), an important feature necessary to avoid uncaging diazo-2 with this light. In each cell, fluorescence was corrected for cross talk between excitation and emission paths by subtracting from the cell signal the mean of the signal measured under identical conditions, but in the cell's absence. To assure that fluorescence intensity signaled only  $\text{Ca}^{2+}$  concentration in the outer segment, fluorescence excitation light was restricted to the outer segment alone with the use of an aperture that created an  $18\text{-}\mu\text{m}$  diameter circle of light centered on the outer segment (Ohyama, T., D.H. Hackos, S. Frings, V. Hagen, U.B. Kaupp, and J.I. Korenbrot, manuscript submitted for publication).

To uncage diazo-2, we delivered the light of a Xe flash (200 J, 0.3-ms duration at half-peak) (Chadwick-Helmuth) by focusing the lamp's arc onto a single cone using the same microscope objective used to visualize the cell. Uncaging light was spectrally selected below 400 nm using optical filters (Hoya Filters). Uncaging and measurement of the consequent changes in membrane current and fluorescence began 3 min after achieving whole cell mode, a sufficient time for equilibration of small molecules, as evidenced by attainment of steady state cell bis-fura2 fluorescence intensity. Experiments were completed within the following 3–5

min. After that time, loss of the modulator was apparent by drift in current amplitude and weakening of the effects of uncaging light.

### Data Analysis

Selected functions were fit to experimental data using nonlinear, least square minimization algorithms (Origin; Microcal Software). Experimental uncertainty throughout is presented as standard deviation. Simulations were executed with dynamic simulation software (Tutsim; Actuality Corp.).

## RESULTS

We measured the  $\text{Ca}^{2+}$  dependence of ligand sensitivity in cGMP-gated currents of electropermeabilized, single cones (ep-cones). In this preparation, outer segment membrane currents are measured with suction electrodes at 0-mV holding potential. To generate an electromotive force that drives the cGMP-gated currents,

measurements are conducted under an ion concentration gradient with  $\text{Na}^+$ , a permeable cation, in the extracellular medium and choline<sup>+</sup>, an impermeant cation, in the intracellular medium. Also, there is only 1  $\mu\text{M}$   $\text{Ca}^{2+}$  in the extracellular medium to reduce the ion's influx through open CNG, and thus to minimize intracellular  $\text{Ca}^{2+}$  loading. Under these conditions, activation of cyclic nucleotide-gated channels generates a sustained, inward current (Fig. 1).

$\text{Ca}^{2+}$ -dependent CNG current modulation in cones is mediated by the interaction of the CNG channel protein with a diffusible, unidentified factor (Rebrik and Korenbrot, 1998). This factor washes out from the ep-cones at rates that accelerate as  $\text{Ca}^{2+}$  concentration declines (Rebrik and Korenbrot, 1998). To define the equilibrium features of the interaction of  $\text{Ca}^{2+}$ , cyclic nucleotides, the channels, and their modulator, the

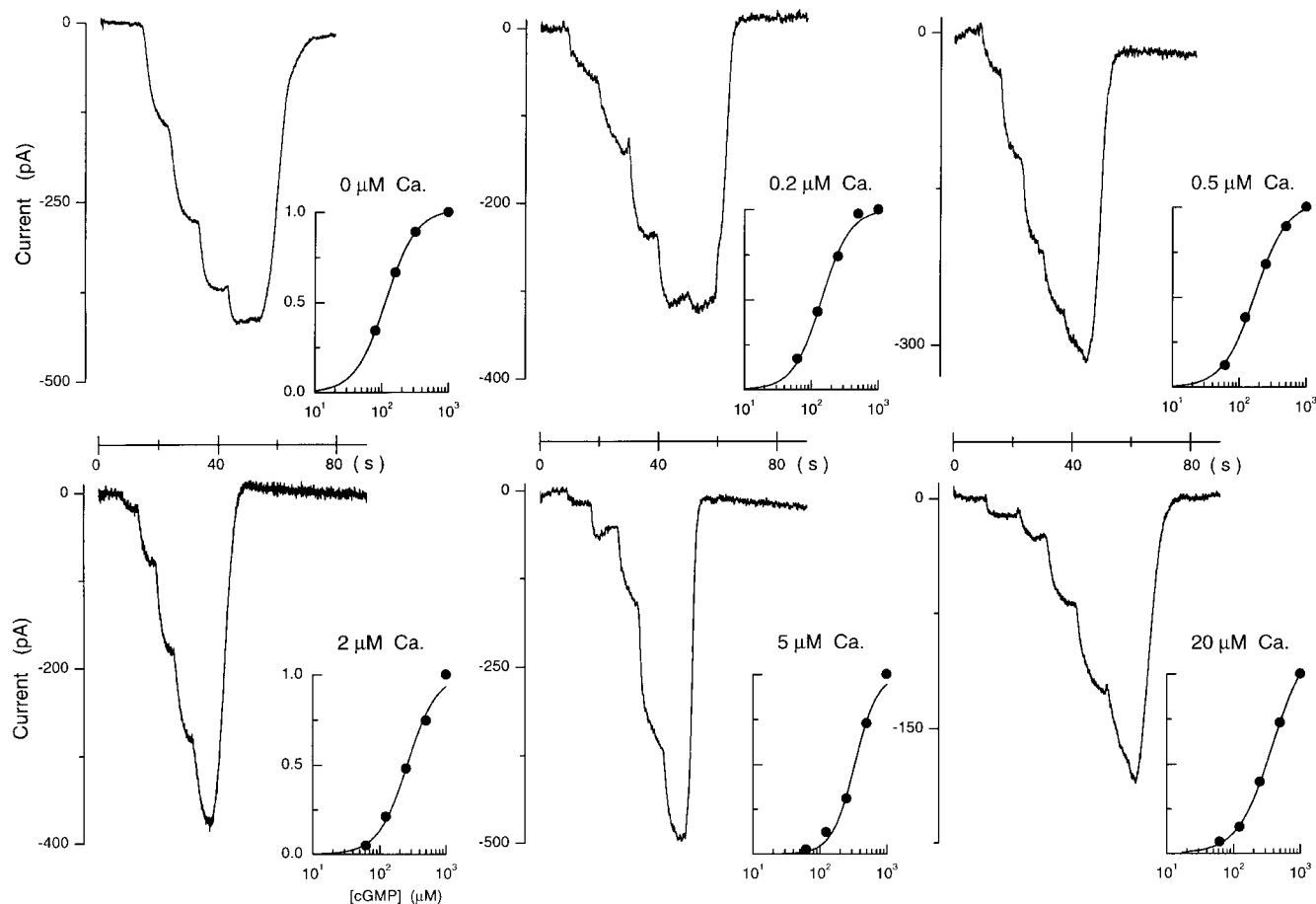


FIGURE 1. Activation of cGMP-dependent currents in the intact outer segment of electropermeabilized cones. In each panel are shown inward outer-segment currents activated by step increments in cytoplasmic cGMP concentrations. Data in each panel were measured in different cells and measurements were completed within 180 s of the moment of electropermeabilization. Each panel illustrates data measured in the presence of different  $\text{Ca}^{2+}$  concentrations between 0 and 20  $\mu\text{M}$ , as labeled. Solutions also included constant concentrations of  $\text{Mg}^{2+}$  (1 mM) and Zaprinast (0.4 mM), a phosphodiesterase inhibitor. cGMP concentrations tested at 0  $\text{Ca}^{2+}$  were 0, 80, 160, 320, and 1,000  $\mu\text{M}$ . At all other  $\text{Ca}^{2+}$  concentrations, cGMP tested were 0, 62.5, 125, 250, 500, and 1,000  $\mu\text{M}$ . The data in each panel are analyzed to illustrate the dependence of peak current amplitude on cGMP. The continuous lines are Hill functions (Eq. 1) optimally fit to the experimental data. For the data shown: at 0  $\mu\text{M}$   $\text{Ca}^{2+}$ ,  $K_{1/2} = 112 \mu\text{M}$  and  $n = 2.0$ ; at 0.2  $\mu\text{M}$   $\text{Ca}^{2+}$ ,  $K_{1/2} = 141.5 \mu\text{M}$  and  $n = 2.1$ ; at 0.5  $\mu\text{M}$   $\text{Ca}^{2+}$ ,  $K_{1/2} = 171 \mu\text{M}$  and  $n = 1.8$ ; at 2  $\mu\text{M}$   $\text{Ca}^{2+}$ ,  $K_{1/2} = 259.8$  and  $n = 1.98$ ; at 5  $\mu\text{M}$   $\text{Ca}^{2+}$ ,  $K_{1/2} = 295 \mu\text{M}$  and  $n = 2.5$ ; and at 20  $\mu\text{M}$   $\text{Ca}^{2+}$ ,  $K_{1/2} = 331 \mu\text{M}$  and  $n = 2.15$ .

concentrations of the interacting components must be constant. To maintain stationary conditions as well as possible, in spite of the potential loss of the modulator, we electroporated the cones in the presence of the solution to be tested, completed all measurements within 180 s of electroporation, and tested only a single  $\text{Ca}^{2+}$  concentration in each cell.

#### *Ca<sup>2+</sup> Dependence of Cyclic Nucleotide Sensitivity in Electroporated Cones*

The dependence of membrane current on cytoplasmic cGMP in dark-adapted ep-cones in the presence of varying concentrations of cytoplasmic  $\text{Ca}^{2+}$  is illustrated in Fig. 1. All solutions contained 1 mM free  $\text{Mg}^{2+}$  and 0.4 mM Zaprinast, an effective inhibitor of cone cGMP-specific phosphodiesterase (PDE) (Gillespie and Beavo, 1989). To compare data among many cells, we normalized current amplitude by dividing the current measured at each cGMP concentration tested by the maximum current measured in the same cell. As described before (Haynes and Yau, 1990; Picones and Korenbrot, 1992), the current amplitude increases with cGMP with a dependence well described by the Hill equation:

$$\frac{I(\text{cGMP})}{I_{\max}} = \frac{[\text{cGMP}]^n}{[\text{cGMP}]^n + K_{1/2}^n}, \quad (1)$$

where  $I$  is the current amplitude measured at the cGMP concentration, cGMP.  $I_{\max}$  is the maximum current measured,  $K_{1/2}$  is the cGMP concentration at which  $I$  has the value  $I_{\max}/2$ , and  $n$  is an adjustable parameter that denotes cooperative interactions. The same function applied to data measured in the presence of all  $\text{Ca}^{2+}$  concentrations tested, but the values of  $K_{1/2}$  (and not  $n$ ) changed with  $\text{Ca}^{2+}$ .

To analyze  $\text{Ca}^{2+}$  dependence in detail, we determined the value of  $K_{1/2}$  in the presence of  $\text{Ca}^{2+}$  at concentrations between 0 and 20  $\mu\text{M}$ . Each  $\text{Ca}^{2+}$  concentration was tested in a different cone and  $K_{1/2}$  values were averaged (Fig. 2).  $\text{Ca}^{2+}$  dependence is well described by a modified Michaelis-Menten equation:

$$K_{1/2}(\text{Ca}) = (K_{1/2}^{\text{hi}} - K_{1/2}^{\text{low}}) \frac{[\text{Ca}]}{[\text{Ca}] + {}^{\text{Ca}}K_m} + K_{1/2}^{\text{low}} \quad (2)$$

where  $K_{1/2}(\text{Ca}^{2+})$  is the value of  $K_{1/2}$  at a given  $\text{Ca}^{2+}$  concentration.  $K_{1/2}^{\text{hi}}$  and  $K_{1/2}^{\text{low}}$  are the extreme values of  $K_{1/2}$ , at 20 and 0  $\mu\text{M}$   $\text{Ca}^{2+}$ , respectively.  ${}^{\text{Ca}}K_m$  is the  $\text{Ca}^{2+}$  concentration at the midpoint between  $K_{1/2}^{\text{hi}}$  and  $K_{1/2}^{\text{low}}$ . The values of  $K_{1/2}$ , their errors, and details of the statistical universe sampled are presented in Table I. Optimum fit of the Michaelis-Menten equation (Eq. 2) to the mean of the data was obtained with  ${}^{\text{Ca}}K_m = 857 \pm 68$  nM.

To insure that the effects reported for cGMP are not confounded by the possible hydrolysis of cGMP by PDE in the outer segment (in spite of the presence of Zapri-

TABLE I  
*Agonist Sensitivity of cGMP-gated Currents in Electroporated Single Cones at Different Ca<sup>2+</sup> Concentrations*

Ca <sup>2+</sup>	cGMP			8Br-cGMP		
	K <sub>1/2</sub>	n	N	K <sub>1/2</sub>	n	N
$\mu\text{M}$	$\mu\text{M}$			$\mu\text{M}$		
0	120.6 ± 9.3	2.01 ± 0.3	20	14.7 ± 0.66	1.4 ± 0.38	4
0.2	157.1 ± 19.8	2.47 ± 0.41	6			
0.5	197.4 ± 55.8	2.07 ± 0.32	15	32.9 ± 3.2	1.42 ± 0.24	3
1				44.9 ± 4.9	1.49 ± 0.23	3
2	265.1 ± 21.8	2.21 ± 0.31	9	57.4 ± 3.7	1.4 ± 0.13	3
5	312.2 ± 84.7	2.19 ± 0.39	9	65.5 ± 7.75	1.8 ± 0.5	3
20	316.4 ± 43.9	2.11 ± 0.49	16	71.1 ± 16.4	1.33 ± 0.18	3

nast), we carried out the same class of measurements using 8Br-cGMP also in the presence of Zaprinast. 8Br-cGMP is an effective activator of cone CNG channels (Hackos and Korenbrot, 1997), but a poor substrate of PDE (Zimmerman et al., 1985). We obtained the same results with 8Br-cGMP as with cGMP (Fig. 3). The normalized current amplitude increased with nucleotide concentration with a dependence well described by the Hill equation. The values of  $K_{1/2}$  changed with  $\text{Ca}^{2+}$  with a dependence well described by the modified Michaelis-Menten equation (Eq. 2) (Fig. 3). The values of  $K_{1/2}$ , their errors, and details of the statistical universe sampled are presented in Table I. Optimum fit of the Michaelis-Menten equation to the mean of the data was obtained with  ${}^{\text{Ca}}K_m = 863 \pm 51$  nM.

#### *Cytoplasmic Loading of Intact Single Cones*

To investigate the time course of the CNG channel modulation, we studied isolated single cones with tight-seal electrodes in the whole-cell mode. The electrode filling solution lacked nucleotide triphosphates and, therefore, cones could not sustain endogenous synthesis of cGMP (Hestrin and Korenbrot, 1987; Rispoli et al., 1993). When the cells' cytoplasm equilibrates fully with the electrode-filling solution, cGMP-gated channels should be inactive and cones should exhibit an outward current at  $-35$  mV because voltage-dependent  $\text{K}^+$  channels in the inner segment should be active (Barnes and Hille, 1989; Maricq and Korenbrot, 1990). Indeed, in the absence of GTP and ATP and 3 min after achieving whole-cell mode, single striped bass cones exhibited an outward current  $21.1 \pm 12.3$  pA ( $n = 35$ ) in amplitude.

To detect CNG channel modulation in the absence of ATP and GTP, we activated the channels with exogenous ligand. We added 8Br-cGMP and 0.4 mM Zaprinast to the electrode-filling solution, which also contained 1 mM diazo-2 and 0.1 mM bis-fura-2 with 1 mM free  $\text{Mg}^{2+}$  and 600 nM free  $\text{Ca}^{2+}$ , a value close to that of  ${}^{\text{Ca}}K_m$  (see above). In Fig. 4, we illustrate typical membrane currents measured in different cones at  $-35$  mV with elec-

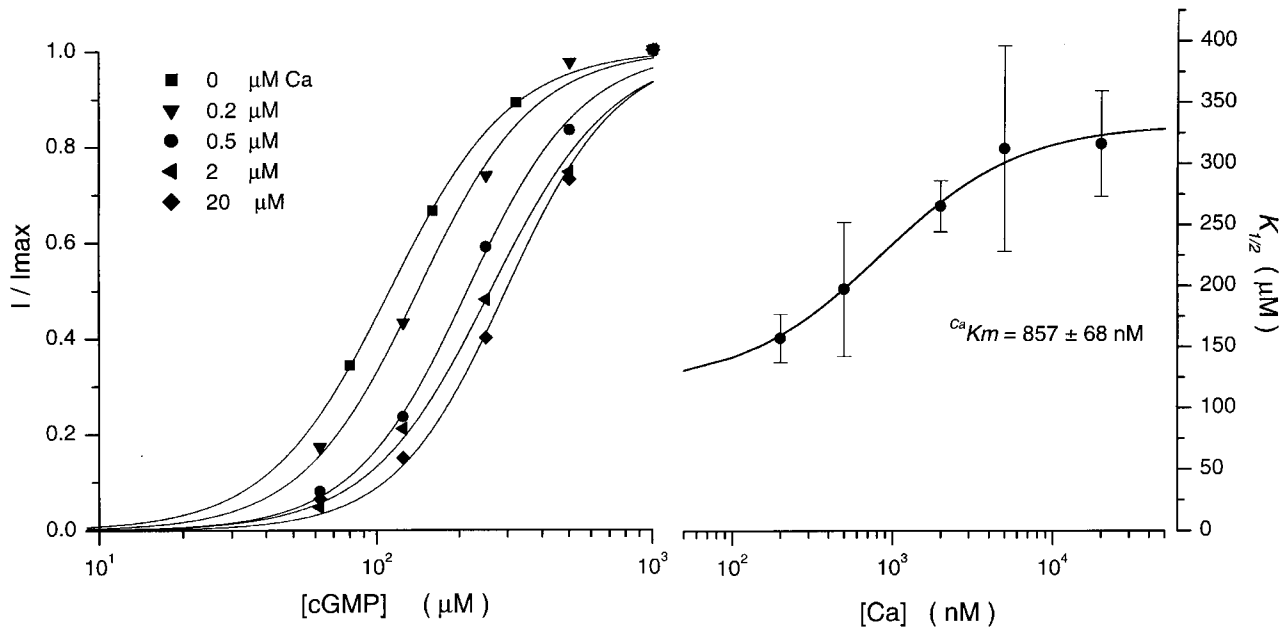


FIGURE 2. cGMP dependence of cone outer segment current as a function of cytoplasmic  $Ca^{2+}$ . (Left) The dependence of normalized current amplitude on cGMP in the presence of various  $Ca^{2+}$  concentrations, as labeled. Each data set was measured in a different ep-cone. The continuous line is the Hill equation that best fits the experimental data. At 0  $\mu M$   $Ca^{2+}$ ,  $K_{1/2} = 112$   $\mu M$  and  $n = 2.0$ ; at 0.2  $\mu M$   $Ca^{2+}$ ,  $K_{1/2} = 141.5$   $\mu M$  and  $n = 2.1$ ; at 0.5  $\mu M$   $Ca^{2+}$ ,  $K_{1/2} = 214$   $\mu M$  and  $n = 2.1$ ; at 2  $\mu M$   $Ca^{2+}$ ,  $K_{1/2} = 259.8$  and  $n = 1.98$ ; and at 20  $\mu M$   $Ca^{2+}$ ,  $K_{1/2} = 331$   $\mu M$  and  $n = 2.15$ . (Right) The dependence of the  $K_{1/2}$  value of the Hill equation on  $Ca^{2+}$ . The data points are the average ( $\pm$ SD) of measurements in different ep-cones. Complete statistical information is given in Table I. The continuous line is a modified Michaelis-Menten function (Eq. 2) that best fits the experimental data. The value of  $^{Ca}K_m$  is given in the figure.

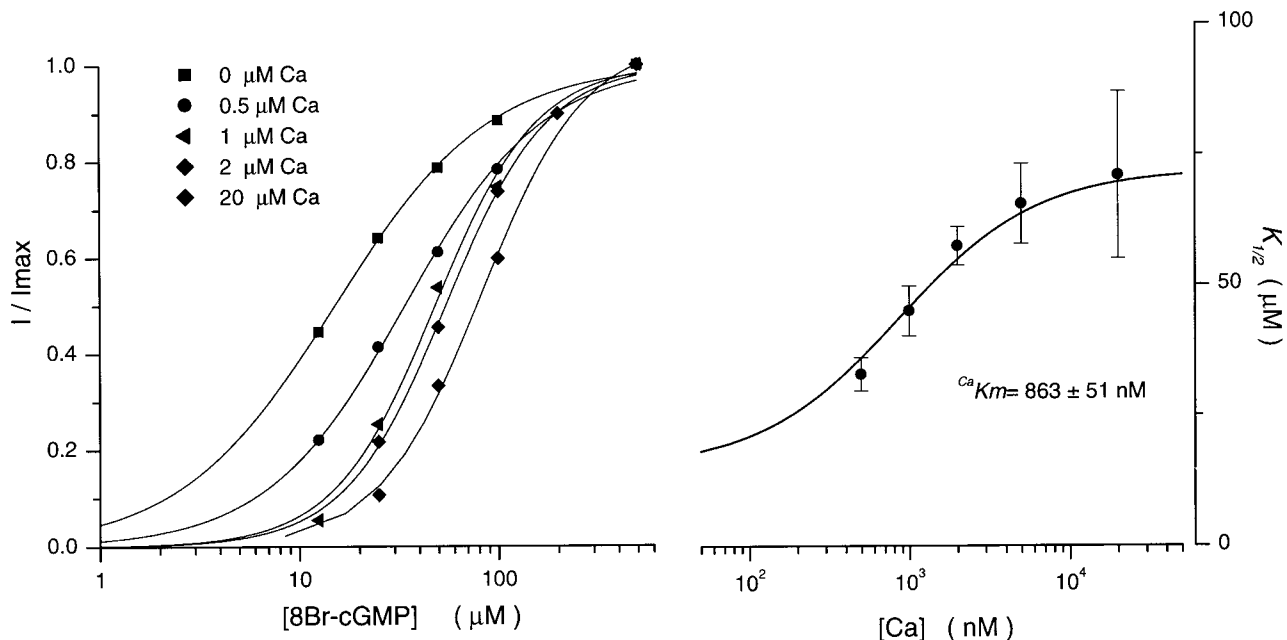


FIGURE 3. 8Br-GMP dependence of cone outer segment current as a function of cytoplasmic  $Ca^{2+}$ . (Left) The dependence of normalized current amplitude on 8Br-cGMP in the presence of various  $Ca^{2+}$  concentrations, as labeled. Each data set was measured in a different ep-cone. The continuous line is the Hill equation that best fits the experimental data. At 0  $\mu M$   $Ca^{2+}$ ,  $K_{1/2} = 15.1$   $\mu M$  and  $n = 1.11$ ; at 0.2  $\mu M$   $Ca^{2+}$ ,  $K_{1/2} = 37.6$   $\mu M$  and  $n = 1.1$ ; at 0.5  $\mu M$   $Ca^{2+}$ ,  $K_{1/2} = 49.5$   $\mu M$  and  $n = 1.67$ ; at 2  $\mu M$   $Ca^{2+}$ ,  $K_{1/2} = 57.2$  and  $n = 1.6$ ; and at 20  $\mu M$   $Ca^{2+}$ ,  $K_{1/2} = 77$   $\mu M$  and  $n = 1.8$ . (Right) The dependence of the  $K_{1/2}$  value of the Hill equation on  $Ca^{2+}$ . The data points are the average ( $\pm$ SD) of measurements in different ep-cones. Complete statistical information is given in Table I. The continuous line is a modified Michaelis-Menten function (Eq. 2) that best fits the experimental data.

trode filled with solution containing either 15 or 30  $\mu\text{M}$  8Br-cGMP. After attaining whole-cell mode, an inward current developed slowly that reached a peak and then declined to a stationary value. This time course reflects the activation of the outer segment inward current as the nucleotide loads the cell and cGMP-gated channels open, followed by channel block due to increasing cytoplasmic  $\text{Ca}^{2+}$  concentration. Because of this associated cytoplasmic  $\text{Ca}^{2+}$  load, we elected to carry out these experiments in a Ringers' solution containing 0.1 mM  $\text{Ca}^{2+}$ , rather than the normal 1 mM. This allowed us to maintain cytoplasmic  $\text{Ca}^{2+}$  within reasonable bounds.

With 15  $\mu\text{M}$  8Br-cGMP in the electrode, the time for current to reach peak had an average value of  $15.8 \pm 2.4$  s ( $n = 8$ , range 13.3–20 s). The decay from peak to steady state values was well described by a single exponential with average time constant of  $32.7 \pm 7.6$  s ( $n = 8$ , range 21.4–41.0). The stationary current was, on average,  $-46 \pm 17$  pA for 15  $\mu\text{M}$  8Br-cGMP ( $n = 21$ ) and  $-415 \pm 107$  pA for 30  $\mu\text{M}$  8Br-cGMP ( $n = 8$ ). Since the photocurrent in the bass single cone outer segment at  $-40$  mV is, on average,  $23 \pm 8$  pA in amplitude (Miller and Korenbrot, 1993), the extent of steady state CNG channel activation by 15  $\mu\text{M}$  8Br-cGMP is close to that in the normal, dark-adapted cell.

#### *Ca<sup>2+</sup>-dependent CNG Channel Modulation in the Intact Cone*

We caused a rapid ( $\ll 50$  ms, see below) decrease in cytoplasmic  $\text{Ca}^{2+}$  by uncaging diazo-2 in intact cone outer segment. In the presence of 15  $\mu\text{M}$  cytoplasmic 8Br-cGMP, the uncaging flash caused a slow increase in current that reached a peak and then slowly returned towards its starting value (Fig. 5). Within the first 6–8 min after establishing whole-cell mode, responses of

similar features could be generated repeatedly by simply waiting  $\sim 2$  min between flashes. After longer intervals, the responses became smaller and even disappeared. The change and eventual loss of the response is almost certainly due to the slow and irreversible loss of modulator, just as occurs in the ep-cones. Data presented here were collected in the interval between 3 and 6 min after achieving whole-cell mode.

In the presence of constant 8Br-cGMP, the increase in current caused by uncaging diazo-2 can reflect  $\text{Ca}^{2+}$ -dependent modulation of channel sensitivity as proposed here, but other mechanisms could also explain the finding. For example: (a)  $\text{Ca}^{2+}$ -dependent activation of guanylyl cyclase (GC), which in turn synthesizes cGMP; (b) activation of  $\text{Ca}^{2+}$ -dependent currents that are not cyclic nucleotide gated; and (c) a direct effect of light. The GC hypothesis is most unlikely because the cones were intentionally made free of nucleotide triphosphates and, without GTP, GC cannot synthesize cGMP. The absence of endogenous cGMP is made evident by the fact that in darkness and in the absence of GTP and ATP, cGMP-gated channels close and the holding current at  $-35$  mV drifts from a starting value near zero to a steady state value of  $21.1 \pm 12.3$  pA ( $n = 35$ ) (due to the activity of voltage-gated  $\text{K}^+$  channels, as discussed above). Moreover, under these conditions, dark-adapted cones do not respond to light, however bright it may be.

To test that the flash-generated current is indeed caused by CNG channel modulation, we tested the response to uncaging flashes in cones loaded with solutions modified as follows: (a) free of 8Br-cGMP (to test whether a cyclic nucleotide-independent current is activated by lowering  $\text{Ca}^{2+}$ ) and (b) diazo-2 replaced by 1 mM BAPTA (to test whether light alone, in the absence

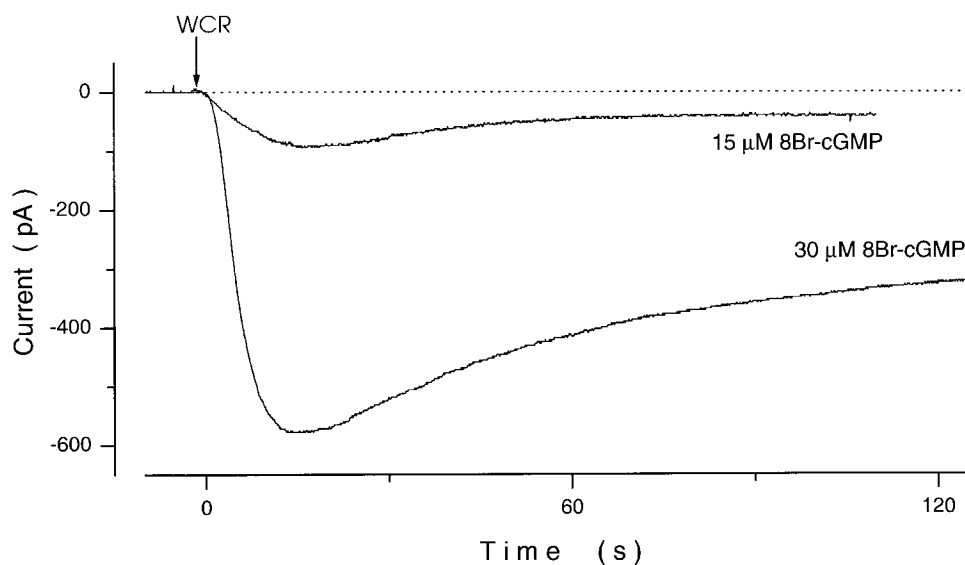


FIGURE 4. Rate of equilibration between cone outer segment cytoplasm and lumen of tight-seal electrode. Shown are whole-cell membrane currents measured in two different cones at  $-35$ -mV holding voltage. At the arrow mark (WCR) (time = 0), whole-cell mode was attained and the contents of the cell cytoplasm began to exchange with the solution filling the tight-seal electrode. This solution contained either 15 or 30  $\mu\text{M}$  8Br-cGMP, as labeled, and 1 mM diazo-2, 1 mM free  $\text{Mg}^{2+}$ , and 600 nM free  $\text{Ca}^{2+}$  (see text for details). As the cyclic

nucleotide loaded the cell, CNG channels in the outer segment were activated and an inward current developed. The current reached a stationary value after  $\sim 2$  min, indicating concentration equilibrium between cell cytoplasm and the electrode lumen.

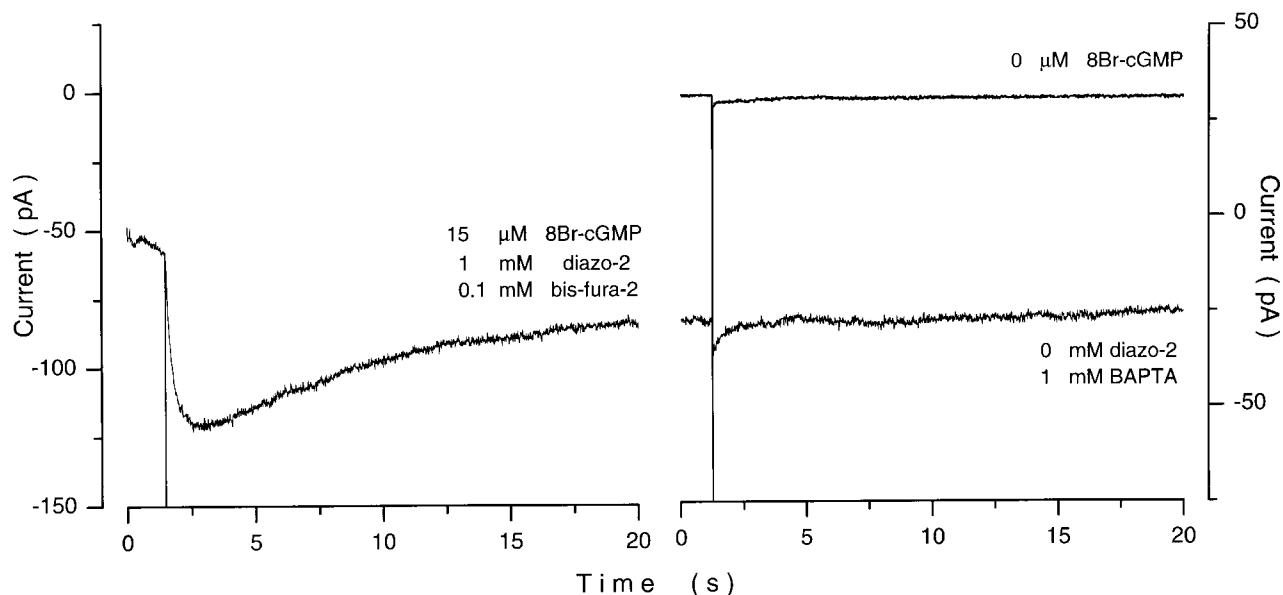


FIGURE 5. Time course of  $\text{Ca}^{2+}$ -dependent CNG current modulation and control experiments. (Left) Whole-cell membrane current measured at  $-35\text{-mV}$  holding voltage in a single cone loaded with standard electrode-filling solution containing  $15\ \mu\text{M}$  8Br-cGMP,  $0.4\ \text{mM}$  Zaprinast,  $1\ \text{mM}$  diazo-2,  $0.1\ \text{mM}$  bis-fura-2 with  $600\ \text{nM}$  free  $\text{Ca}^{2+}$ , and  $1\ \text{mM}$  free  $\text{Mg}^{2+}$ .  $1.5\ \text{s}$  after starting the record, at the time indicated by the spike in the record, a Xenon flash uncaged diazo-2, causing a slow increase in the inward current that reached a peak in  $\sim 1.4\ \text{s}$ , and then returned towards its starting value. At the peak, membrane conductance was enhanced 2.26-fold. (Right) Currents measured at  $-35\ \text{mV}$  in two different cones, each loaded with a modified electrode-filling solution. Two control conditions were tested: (a) omitting 8Br-cGMP ( $0\ \mu\text{M}$  8Br-cGMP), and (b) replacing diazo-2 with  $1\ \text{mM}$  BAPTA ( $0\ \mu\text{M}$  Diazo-2). Free  $\text{Ca}^{2+}$  and  $\text{Mg}^{2+}$  remained at  $600\ \text{nM}$  and  $1\ \text{mM}$ , respectively. In the absence of 8Br-cGMP, the net current was outward because CNG channels are closed and current flows through voltage-gated  $\text{K}^+$  channels in the cone inner segment. The uncaging flash did not cause a current change in either of the control experiments.

of  $\text{Ca}^{2+}$  changes can cause channel activation). Typical results of these tests are shown in Fig. 5. In the absence of 8Br-cGMP, the holding current at  $-35\ \text{mV}$  was outward,  $21.1 \pm 12.3\ \text{pA}$  ( $n = 35$ ), and reflects the activity of voltage-dependent  $\text{K}^+$  channels in the inner segment. Uncaging flashes caused a decrease in  $\text{Ca}^{2+}$ , but failed to generate changes in current. In the absence of diazo-2,  $15\ \mu\text{M}$  8Br-cGMP sustained a stationary inward current and light flashes also failed to change the current. The same occurred in every cell we tested (8Br-cGMP free,  $n = 4$ ; diazo-2 free,  $n = 5$ ). Also, adding  $10\ \text{mM}$  BAPTA to the electrode-filling solution blocked the flash-generated current change (data not shown). Examination of the data, however, shows a large and very fast spike at the moment of flash (Figs. 5–7). The spikes are inevitable artifacts caused by the high-energy discharge of the capacitors in the Xe flash instrument. Thus, control experiments indicate that the slow change in current generated by uncaging diazo-2 arise specifically from activation of cyclic nucleotide-gated current caused by lowering cytoplasmic  $\text{Ca}^{2+}$ .

#### *Time Course of Flash-generated Sequestration of Cytoplasmic $\text{Ca}^{2+}$*

The electrode-filling solution was buffered with dark diazo-2 and bis-fura-2 to attain  $1\ \text{mM}$  free  $\text{Mg}^{2+}$  and  $600\ \text{nM}$  free  $\text{Ca}^{2+}$ ; however, the effective  $\text{Ca}^{2+}$  concentra-

tion in the cone outer segment may differ from this value because of the action of endogenous mechanisms that control cytoplasmic  $\text{Ca}^{2+}$  (Yau and Nakatani, 1985; Miller and Korenbrot, 1987; Lagnado et al., 1992). Chemical measurements have demonstrated that in the absence of buffers, uncaging diazo-2 fully sequesters  $\text{Ca}^{2+}$  within  $2\ \text{ms}$  after a flash (Adams et al., 1989). In the cytoplasmic space and in the presence of endogenous and exogenous buffers, the kinetics of  $\text{Ca}^{2+}$  sequestration by uncaging diazo-2 could be different and must be experimentally determined.

To determine the speed of  $\text{Ca}^{2+}$  sequestration in a single cone outer segment caused by uncaging diazo-2, we measured the fluorescent signal of cytoplasmic bis-fura-2 excited at  $380\ \text{nm}$  and emitted in the range between  $410$  and  $600\ \text{nm}$ . Under these conditions, a decrease in  $\text{Ca}^{2+}$  causes an increase in fluorescence intensity. Fluorescence intensity signaled only free  $\text{Ca}^{2+}$  in the outer segment because an optical aperture restricted fluorescence excitation light to the outer segment alone. Fig. 6 illustrates a typical result in a cone loaded with  $15\ \mu\text{M}$  8Br-cGMP (with Zaprinast). In the absence of an uncaging flash, cell fluorescence intensity was constant, indicating a steady  $\text{Ca}^{2+}$  concentration unaffected by the  $380\text{-nm}$  fluorescence excitation light. This is important because it demonstrates that the fluorescence monitoring light alone did not uncage diazo-2. Presentation of

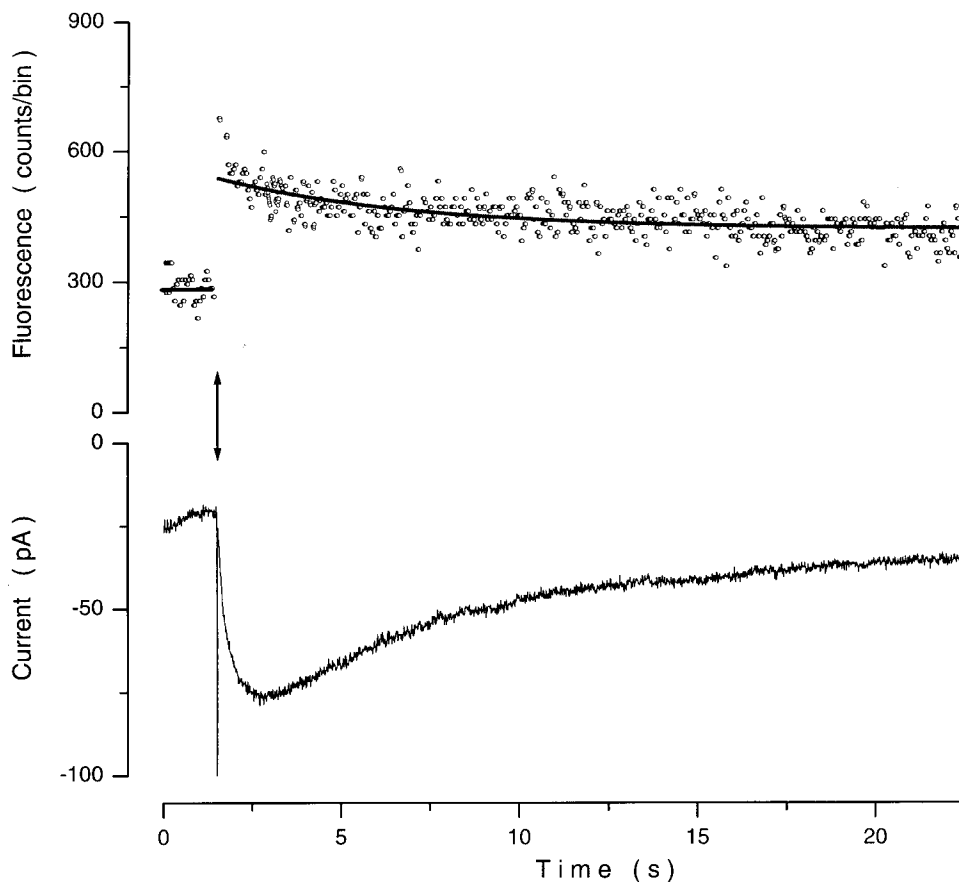


FIGURE 6. Time course of changes in membrane current and cytoplasmic  $\text{Ca}^{2+}$  concentration in a cone outer segment caused by uncaging diazo-2. The single cone was loaded with standard electrode-filling solution containing 15  $\mu\text{M}$  8Br-cGMP, 0.4 mM Zaprinast, 1 mM diazo-2, 0.1 mM bis-fura-2 with 600 nM free  $\text{Ca}^{2+}$  and 1 mM free  $\text{Mg}^{2+}$ . 1.5 s after starting the record, at the time indicated by the double-ended arrowhead in the record, a Xenon flash uncaged diazo-2. (Top) The fluorescence excited at 380 nm and emitted in the 410–600-nm range. A rise in fluorescence intensity indicates that uncaging diazo-2 caused a rapid initial decrease in  $\text{Ca}^{2+}$  concentration, which then slowly drifted back towards its starting value. (○) Data in counts per 50-ms bin. The continuous line depicts the analytical function (Eq. 3) that optimally describes the time course of  $\text{Ca}^{2+}$  concentration change. (Bottom) The whole-cell membrane current at  $-35\text{-mV}$  holding voltage measured simultaneously. The sudden  $\text{Ca}^{2+}$  sequestration caused a slow 3.75-fold increase in membrane conductance that reached to a peak in  $\sim 1.35$  s.

an uncaging flash caused an instantaneous increase in fluorescence, which then slowly recovered towards its starting value (Fig. 6). The increase in fluorescence indicates that  $\text{Ca}^{2+}$  concentration decreased within 50 ms of the flash. This value, however, is an upper limit on the actual speed of sequestration imposed by the bandwidth of the photon counting instrumentation.  $\text{Ca}^{2+}$  reached a minimum, and then slowly recovered, presumably because of additional  $\text{Ca}^{2+}$  influx through the newly activated CNG channels.

We found that in all cells tested the  $\text{Ca}^{2+}$  concentration change caused by uncaging diazo-2 was well described by an exponential process (Fig. 6):

$$\text{Ca}^{2+}(t) = \text{Ca}_{\text{dark}}^{2+} - \text{Ca}_{\text{ss}}^{2+} - [(\text{Ca}_{\text{peak}}^{2+} - \text{Ca}_{\text{ss}}^{2+})\exp(-t/\tau_{\text{Ca}})], \quad (3)$$

where  $\text{Ca}_{\text{dark}}^{2+}$  is the concentration preceding the flash,  $\text{Ca}_{\text{peak}}^{2+}$  is the maximum decrease in concentration, and  $\text{Ca}_{\text{ss}}^{2+}$  is the concentration at the end of the sampling period (23 s after the uncaging flash).  $t = 0$  is the moment the flash is presented and is the time constant of decline between the peak and ss values. We note that ss is not truly a stationary value; 2–3 min after a flash,

$\text{Ca}^{2+}$  concentration returned to its original “dark” value. This very slow recovery is expected from the eventual equilibrium between cell cytoplasm and electrode lumen.

We did not calibrate in situ the 380-nm bis-fura-2 fluorescence in absolute units of  $\text{Ca}^{2+}$  concentration, a difficult task that is even less reliable when only a single excitation wavelength is used (Williams and Fay, 1990). Concentration changes in each cell, however, could be expressed in units of  $\text{Ca}_{\text{dark}}^{2+}$  by dividing changes in fluorescence by the intensity measured in the same cell before the uncaging flash. The flash-generated  $\text{Ca}^{2+}$  concentration changes and their time course were remarkably similar among different cells. For nine cones,  $\text{Ca}_{\text{peak}}^{2+}/\text{Ca}_{\text{dark}}^{2+} = 0.52 \pm 0.07$ ,  $\text{Ca}_{\text{ss}}^{2+}/\text{Ca}_{\text{dark}}^{2+} = 0.70 \pm 0.08$ , and  $\tau_{\text{Ca}} = 5.38 \pm 0.35$  s.

#### A Kinetic Model of CNG Channel Modulation

Examination of the data in Figs. 5 and 6, each a different cone, shows that, after an uncaging flash, cytoplasmic  $\text{Ca}^{2+}$  changed more rapidly than did the membrane current. The difference in the early time course of the fluorescent and current signals is illustrated in detail in Fig. 7, data measured in yet a different cone.

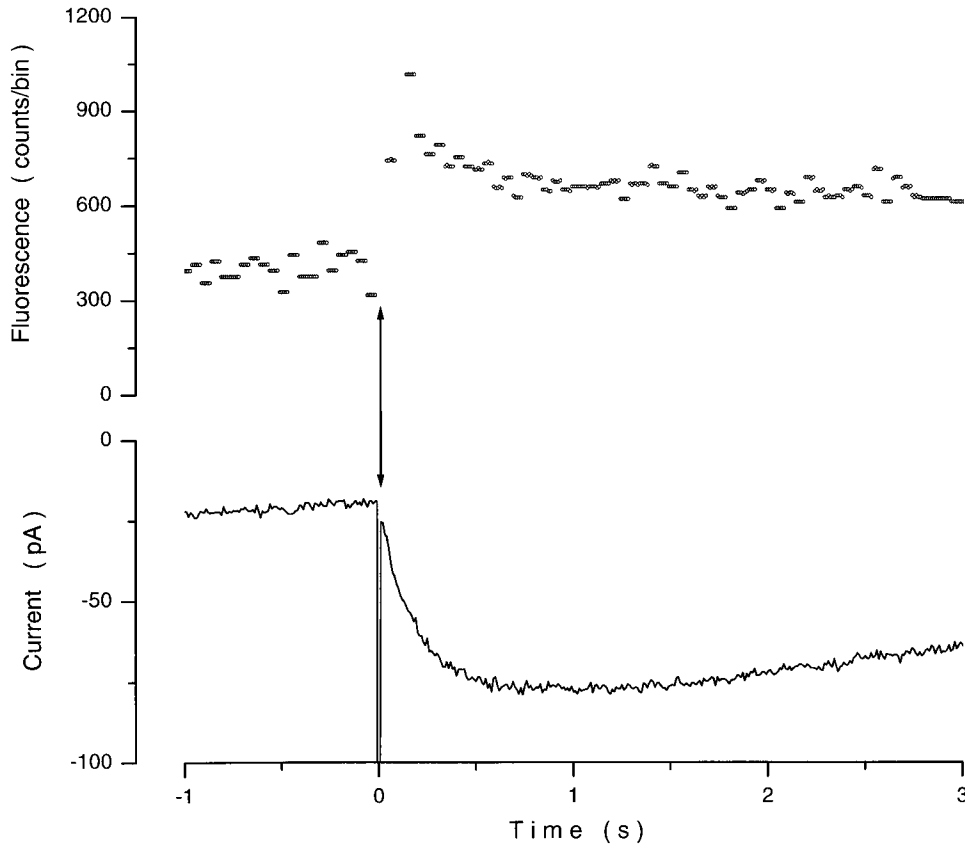
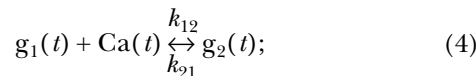


FIGURE 7. High time resolution of the initial time course of changes in membrane current and cytoplasmic  $\text{Ca}^{2+}$  concentration in a cone outer segment caused by uncaging diazo-2. The single cone was loaded with standard electrode-filling solution containing  $15 \mu\text{M}$  8Br-cGMP,  $0.4 \text{ mM}$  Zaprinast,  $1 \text{ mM}$  Diazo-2,  $0.1 \text{ mM}$  bis-fura-2 with  $600 \text{ nM}$  free  $\text{Ca}^{2+}$ , and  $1 \text{ mM}$  free  $\text{Mg}^{2+}$ . (Top) The outer segment fluorescence excited at  $380 \text{ nm}$  and emitted in the  $410\text{--}600 \text{ nm}$  range; (bottom) the membrane current measured simultaneously at  $-35\text{-mV}$  holding voltage. At time  $t = 0$ , the uncaging flash was delivered causing a rapid ( $<50 \text{ ms}$ ) loss of cytoplasmic  $\text{Ca}^{2+}$  and a much slower change in membrane current. The sudden  $\text{Ca}^{2+}$  sequestration caused a slow fourfold increase in membrane conductance that reached to a peak in  $\sim 0.95 \text{ s}$ .

After an uncaging flash,  $\text{Ca}^{2+}$  concentration reached its minimum within  $50 \text{ ms}$ , yet current increased with an exponential time course and reached a peak only after  $\sim 0.9 \text{ s}$ . At the peak, the nucleotide-gated conductance was enhanced 3.85-fold. In seven cells,  $\text{Ca}^{2+}$  was always minimal within  $50 \text{ ms}$ , and current reached peak in a mean time of  $1.25 \pm 0.23 \text{ s}$ . Conductance enhancement at the peak was, on average,  $2.33 \pm 0.95$ -fold.

We developed a kinetic model that successfully matched experimental data. Let us simply assume that CNG channels exist at concentration  $g_1$  in conductance state S. Conductance state is the product of single channel conductance and probability of opening. Thus, membrane conductance is the product of  $g_1$  and S. Upon  $\text{Ca}^{2+}$  binding, and in the presence of the modulator, the channels change to a new concentration  $g_2$  of conductance state S. Membrane conductance changes as channel concentration changes from  $g_1$  to  $g_2$ . We do not specify the molecular mechanisms underlying the change in channel concentration (and, therefore, membrane conductance), we simply assume that concentration change is pseudo first order, characterized by a time constant  $\tau_g$  (Gutfreund, 1995) (Eq. 4):



then, when  $g_1(0) \gg \text{Ca}(t)$  (Eq. 5):

$$\frac{dg_2(t)}{dt} = \frac{1}{\tau_g} [\text{Ca}(t) - g_2(t)], \quad (5)$$

where (Eq. 6):

$$\tau_g = [k_{12}g_1(0) + k_{21}]^{-1} \quad (6)$$

and  $\text{Ca}(t)$  is the  $\text{Ca}^{2+}$  concentration given by Eq. 3.

To test the adequacy of the model, we fit data simulated by the model to experimental results. To this end, and for each set of experimental data: (a) we fit Eq. 3 to the measured fluorescence change and used the resulting analytical expression to describe  $\text{Ca}(t)$  for that data set. (b) We simulated changes in membrane conductance using the model above; the simulation predicts the change in conductance caused by a defined change  $\text{Ca}^{2+}$  provided as an input. (c) We systematically varied the values of  $\tau_g$  to best match simulated and experimental data. The kinetic model could be made to simulate experimental data well (Fig. 8). For seven cells, with fits of similar quality to that shown in Fig. 8, mean value was  $\tau_g = 0.40 \pm 0.14 \text{ s}$ .

#### DISCUSSION

Activation of cGMP-gated ion channels in intact cone photoreceptors depends on agonist concentration, but their sensitivity, how much agonist is necessary for activation, depends on  $\text{Ca}^{2+}$ . Ligand sensitivity decreases as

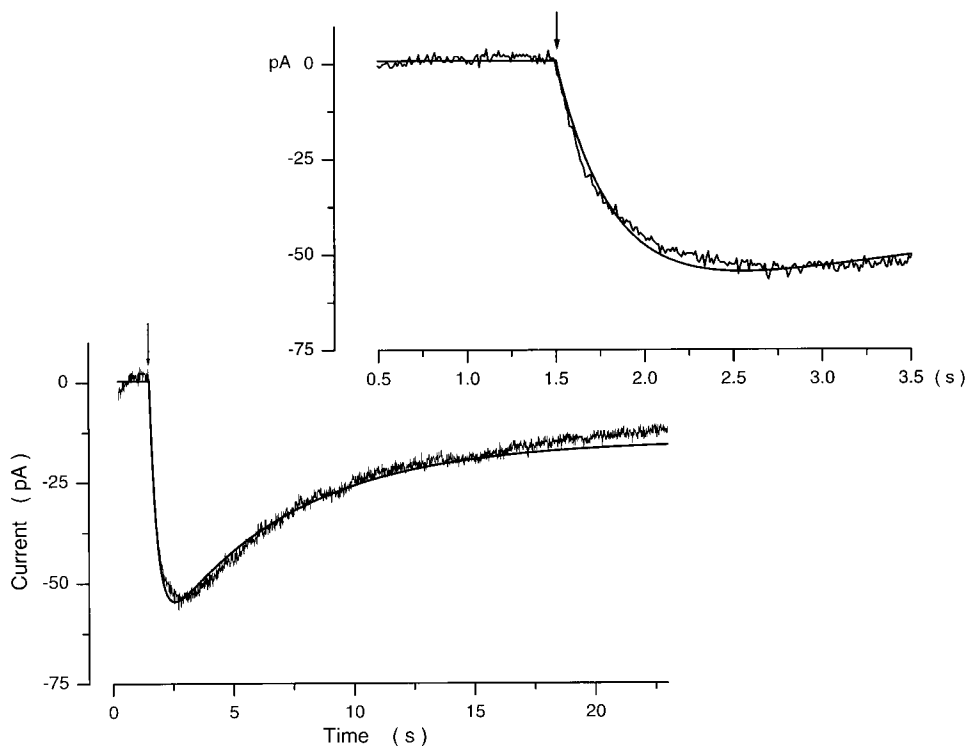


FIGURE 8. Experimental and simulated changes in membrane current caused by sudden  $\text{Ca}^{2+}$  loss in a cone outer segment in the presence of unchanging 8Br-cGMP. Experimental data (noisy traces) are currents measured at  $-35$  mV in a cone loaded with standard electrode-filling solution containing  $15 \mu\text{M}$  8Br-cGMP,  $0.4$  mM Zaprinast,  $1$  mM diazo-2,  $0.1$  mM bis-fura-2 with  $600$  nM free  $\text{Ca}^{2+}$ , and  $1$  mM free  $\text{Mg}^{2+}$ . At the arrow,  $\text{Ca}^{2+}$  was sequestered by uncaging diazo-2. The  $\text{Ca}^{2+}$  concentration change in the cell was measured (not shown) and described by Eq. 3 with  $\text{Ca}_{\text{peak}}^{2+}/\text{Ca}_{\text{dark}}^{2+} = 0.72$ ,  $\text{Ca}_{\text{ss}}^{2+}/\text{Ca}_{\text{dark}}^{2+} = 0.91$ , and  $\tau_{\text{Ca}} = 5.55$  s. Simulated data (smooth traces) are the results of simulations that assume channel modulation is a pseudo-first-order process rate limited by the kinetics of  $\text{Ca}^{2+}$  concentration change, with time constant  $\tau_g = 0.32$  s. The same data are shown at two different time resolutions.

$\text{Ca}^{2+}$  increases, and this relationship is well described by a Michaelis-Menten function (Eq. 2), suggesting that modulation arises from the noncooperative binding of  $\text{Ca}^{2+}$  to a single site. This apparent simplicity belies the fact that the molecular events underlying the  $\text{Ca}^{2+}$ -dependent modulation involve interaction among at least three distinct molecules:  $\text{Ca}^{2+}$  ions, a modulator protein, and the ion channels (themselves constituted by alpha and beta subunits; Gerstner et al., 2000). The interaction likely occurs on the channel's  $\beta$  subunit, by analogy to the case in rod CNG channels (Hsu and Molday, 1994; Grunwald et al., 1998; Weitz et al., 1998). The modulator is a soluble factor that is lost from cones in the absence of  $\text{Ca}^{2+}$  and  $\text{Mg}^{2+}$  (Hackos and Korenbrot, 1997; Rebrik and Korenbrot, 1998). The identity of the modulator has not been established, but it is not calmodulin, since exogenous calmodulin does not mimic its action (Hackos and Korenbrot, 1997; Haynes and Stotz, 1997) and the calmodulin blocker Mastoparan ( $400$  nM) does not block modulation in ep-cones (our unpublished observations).

In the experiments with ep-cones, we minimized the extent of modulator loss by conducting all measurements in the presence of  $1$  mM  $\text{Mg}^{2+}$  and completing them within  $180$  s of inner segment permeabilization. In intact cones under whole-cell voltage clamp, modulator was still lost, but at a much slower rate. We minimized modulator loss in intact cones by completing all measurements in a window between  $3$  and  $6$  min after attaining whole-cell mode. This period was long enough

to allow equilibration between the cell and electrode lumen, and yet not so long as to lose the modulator.

The  $\text{Ca}^{2+}$ -dependent modulation of channel sensitivity, quantitatively expressed by the value of  ${}^{\text{Ca}}K_m$  (Eq. 2) is the same whether channels are activated with cGMP or 8Br-cGMP,  $\sim 860$  nM. This observation is important because it indicates that the interaction between  $\text{Ca}^{2+}$ , modulator, and channel is independent of the ligand gating the channel. In a previous report (Rebrik and Korenbrot, 1998), we measured the  $\text{Ca}^{2+}$  dependence of the cGMP-gated current at a single nucleotide concentration and defined  $K_{\text{Ca}}$  as the  $\text{Ca}^{2+}$  concentration at which the current amplitude was half maximal. That is not the same definition as we have given  ${}^{\text{Ca}}K_m$  here (Eq. 2), a measurement of the  $\text{Ca}^{2+}$  dependence of ligand sensitivity.  $\text{Ca}^{2+}$ -dependent channel modulation in intact rods has been explored only at a single ligand concentration and  $K_{\text{Ca}}$  was found to be  $\sim 50$  nM  $\text{Ca}^{2+}$  (Nakatani et al., 1995; Sagoo and Lagnado, 1996), compared with  $286$  nM for cones (Rebrik and Korenbrot, 1998).  ${}^{\text{Ca}}K_m$  has not been measured in rods. Since the free  $\text{Ca}^{2+}$  in a dark-adapted outer segment is in the range  $400$ – $600$  nM (rods: Korenbrot and Miller, 1989; Gray-Keller and Detwiler, 1994; McCarthy et al., 1994; cones: Sampath et al., 1999), in cones, but not rods, channel modulation is significant in darkness and even small changes in  $\text{Ca}^{2+}$  concentration, as may occur in response to dim lights, will affect channel sensitivity. Channel modulation in rods can be expected to be of consequence only in the presence of bright illumination.

In both rods and cones in the dark, ~3–5% of all cGMP-gated channels are active. Because the ligand sensitivity of the channels in the two receptor types is so different (Rebrik and Korenbrot, 1998), the standing cytoplasmic concentration of cGMP is likely higher in cone than in rod outer segments. If we assume that, in darkness, free cytoplasmic  $\text{Ca}^{2+}$  in both photoreceptors is 600 nM and 3% of the channels are active, then our data indicate that free cGMP concentration is ~10  $\mu\text{M}$  in rod outer segments and 52  $\mu\text{M}$  in cones.

Signal transduction in olfactory neurons arises from odorant-dependent changes in cytoplasmic cAMP, which, in turn, activates specific CNG-gated channels. The ligand sensitivity of these channels decreases with increasing  $\text{Ca}^{2+}$  (Liu et al., 1994; Balasubramanian et al., 1996; Kleene, 1999), and this modulation plays a role in odor adaptation (Kurahashi and Menini, 1997). At first glance, the extent of sensitivity modulation in olfactory CNG channels appears larger than in cones:  $K_{1/2}$  can change by up to ninefold. However, to obtain such a large change,  $\text{Ca}^{2+}$  must change from 0.1  $\mu\text{M}$  to 3 mM. Detailed exploration of  $\text{Ca}^{2+}$  dependence of  $K_{1/2}$  in olfactory neurons reveals one range of changes that plateaus between  $10^{-5}$  and  $10^{-4}$  M  $\text{Ca}^{2+}$  and a second, distinct range at higher  $\text{Ca}^{2+}$  (Kleene, 1999). In the low range of  $\text{Ca}^{2+}$  concentration, which overlaps the range explored in this report, the change in  $K_{1/2}$  in the olfactory neurons is approximately three- to fourfold, not that different from cones.

In the intact cones, we found a relatively large variance in the values of  $K_{1/2}$  at any given  $\text{Ca}^{2+}$  concentration (Table I). Also, the value of  $n$ , while independent of  $\text{Ca}^{2+}$ , differs between cGMP and 8Br-cGMP, as reported before (Rebrik and Korenbrot, 1998). The variance in the value of  $K_{1/2}$  may reflect various states of channel phosphorylation. Native rod channels or recombinant channels formed by homopolymers of alpha subunits alone, demonstrate a range of  $K_{1/2}$  values (Molokanova et al., 1997; Ruiz et al., 1999) that can be changed by phosphorylation/dephosphorylation of a specific tyrosine (Molokanova et al., 1997, 1999). In cone outer segment membrane patches, addition of ATP can change CNG channel sensitivity (Watanabe and Shen, 1997); this phenomenon, however, is observed only some of the time and, though it may arise from CNG channel phosphorylation, inconsistent observations in “detached” outer segment patches can be confounded by the fact that elements of the transducing cascade can remain as part of the patch. While channel ligand sensitivity changes with the state of phosphorylation, little information is now available on whether such channel phosphorylation changes in the course of light responses. It must be noted, however, that accessibility to phosphorylation in homopolymeric alpha subunits changes with gating (Molokanova et al., 1999).

Modulation of  $K_{1/2}$  by phosphorylation has not been definitely demonstrated in cones, but probably occurs. Modulation by phosphorylation, however, is unlikely to play a role in the results presented here since nucleotide triphosphates, both ATP and GTP, were absent from the cells, both in ep-cones and in the whole-cell mode. The lack of nucleotide triphosphates in the intact cones was verified by the fact that holding currents recorded in the absence of 8Br-cGMP were positive, reflecting current flowing out of the cone through voltage-gated  $\text{K}^+$  channels in the inner segment unopposed by the activity of outer segment channels. Absence of triphosphate nucleotide substrates also assured us that  $\text{Ca}^{2+}$ -dependent guanylyl-cyclase was not active in the cones studied in this report.

We measured the kinetics of sensitivity modulation at a fixed ligand concentration, 15  $\mu\text{M}$  8Br-cGMP. We elected this concentration because it activated channels to an extent comparable with that of a normal dark-adapted cone. In the presence of higher 8Br-cGMP concentrations, we observed, in addition to sensitivity modulation, small current changes that reflected flash-induced hydrolysis of the nucleotide. It must be recalled that 8Br-cGMP is a poor substrate of the photoreceptors' PDE when compared with cGMP, but the enzyme can nonetheless hydrolyze it. Indeed, photoresponses can be measured in rods loaded with 8Br-cGMP alone (Cameron and Pugh, 1990).

The time course of the  $\text{Ca}^{2+}$ -dependent change in ligand sensitivity is slower than that of the  $\text{Ca}^{2+}$  change itself. The kinetics of the change in sensitivity is well described as a pseudo-first-order process rate limited by the  $\text{Ca}^{2+}$  concentration change with a time constant of ~0.4 s. The kinetics of most of the  $\text{Ca}^{2+}$ -dependent events in the phototransduction cascade of rods or cones is not known with precision (Calvert et al., 1998). In the absence of specific information, it has been common, and reasonable, to assume that  $\text{Ca}^{2+}$ -limited reactions are “instantaneous” (Miller and Korenbrot, 1994; Nikonov et al., 1998). These assumptions, however, have generally gone unproven and it is important to determine, when possible, the precise kinetics of  $\text{Ca}^{2+}$ -dependent reactions.

In bass single cones, voltage-clamped current responses to dim light flashes reach peak in 80–100 ms and recover fully within 300 ms (Miller and Korenbrot, 1993). Because channel modulation has a relatively slow time constant of response, it is reasonable to expect that channel sensitivity will change little in the activation phase of a single, dim flash response. Channel modulation must be significant in the course of recovery after a dim flash and certainly in response to bright flashes that saturate the photoresponse or steps of light longer than a few seconds at any intensity. While the exact details of the contribution of channel modulation

to the transduction process are yet to be defined, channel modulation may be the first process that can be said to operate as part of the mechanisms that modulate transduction in cones, but not rods.

In bass single cones, as in all cones, the response to a constant dim flash changes as a function of the intensity of background light against which the flash is presented. In general, the peak amplitude decreases as the background intensity rises, and the relationship between peak current and background intensity is described by the Weber law (Miller and Korenbrot, 1993). The time course of the effect of background on the flash response, however, is not instantaneous. A flash presented immediately after the light step generates a small amplitude response. The amplitude of this flash-generated response becomes larger as the interval between the onset of the light step and the presentation of the test flash increases, until an unchanging amplitude response is obtained that follows the Weber law. This process in striped bass cones has an exponential time course of  $\sim 1$ -s time constant (Miller and Korenbrot, 1993). Changes in CNG channel sensitivity occur over this time domain and, therefore, can be expected to play a critical role in this adaptation process.

We thank C. Chung, P. Faillace, A. Picones, A. Olson, T. Ohayama, and C. Paillart for their helpful criticism and continuing interest.

This study was supported in part by a student fellowship supported by the Fight for Sight research division of Prevent Blindness America (E. Kotelnikova) and a Grant-in-Aid of research from the National Academy of Sciences, through Sigma Xi, The Scientific Research Society. Research was also supported by the National Institutes of Health (EY-05498).

Submitted: 22 June 2000

Revised: 21 August 2000

Accepted: 21 August 2000

#### REFERENCES

- Adams, S.R., J.P.Y. Kao, and R.Y. Tsien. 1989. Biologically useful chelators that take up Ca upon illumination. *J. Am. Chem. Soc.* 111: 7957–7968.
- Balasubramanian, S., J.W. Lynch, and P.H. Barry. 1996. Calcium-dependent modulation of the agonist affinity of the mammalian olfactory cyclic nucleotide-gated channel by calmodulin and a novel endogenous factor. *J. Membr. Biol.* 152:13–23.
- Barnes, S., and B. Hille. 1989. Ionic channels of the inner segment of tiger salamander cone photoreceptors. *J. Gen. Physiol.* 94:719–743.
- Bauer, P.J. 1996. Cyclic GMP-gated channels of bovine rod photoreceptors: affinity, density and stoichiometry of  $\text{Ca}^{2+}$ -calmodulin binding sites. *J. Physiol.* 494:675–685.
- Burkhardt, D.A. 1994. Light adaptation and photopigment bleaching in cone photoreceptors in situ in the retina of the turtle. *J. Neurosci.* 14:1091–1095.
- Calvert, P.D., T.W. Ho, Y.M. LeFebvre, and V.Y. Arshavsky. 1998. Onset of feedback reactions underlying vertebrate rod photoreceptor light adaptation. *J. Gen. Physiol.* 111:39–51.
- Cameron, D.A., and E.N. Pugh, Jr. 1990. The magnitude, time course and spatial distribution of current induced in salamander rods by cyclic guanine nucleotides. *J. Physiol.* 430:419–430.
- Chen, C.K., J. Inglese, R.J. Lefkowitz, and J.B. Hurley. 1995.  $\text{Ca}^{2+}$ -dependent interaction of recoverin with rhodopsin kinase. *J. Biol. Chem.* 270:18060–18066.
- Dizhoor, A.M., E.V. Olshevskaia, W.J. Henzel, S.C. Wong, J.T. Stults, I. Ankoudinova, and J.B. Hurley. 1995. Cloning, sequencing, and expression of a 24-kDa  $\text{Ca}^{2+}$ -binding protein activating photoreceptor guanylyl cyclase. *J. Biol. Chem.* 270:25200–25206.
- Fain, G.L. 1976. Sensitivity of toad rods: dependence on wavelength and background illumination. *J. Physiol.* 261:71–101.
- Fain, G.L., and H.R. Matthews. 1990. Calcium and the mechanism of light adaptation in vertebrate photoreceptors. *Trends Neurosci.* 13:378–384.
- Fain, G.L., H.R. Matthews, and M.C. Cornwall. 1996. Dark adaptation in vertebrate photoreceptors. *Trends Neurosci.* 19:502–507.
- Gerstner, A., X. Zong, F. Hofmann, and M. Biel. 2000. Molecular cloning and functional characterization of a new modulatory cyclic nucleotide-gated channel subunit from mouse retina. *J. Neurosci.* 20:1324–1332.
- Gillespie, P.G., and J.A. Beavo. 1989. Inhibition and stimulation of photoreceptors phosphodiesterase by dipyrindamole and M&B 22,948. *Mol. Pharmacol.* 36:773–781.
- Gordon, S.E., J. Downing-Park, and A.L. Zimmerman. 1995. Modulation of the cGMP-gated ion channel in frog rods by calmodulin and an endogenous inhibitory factor. *J. Physiol.* 486:533–546.
- Gray-Keller, M.P., and P.B. Detwiler. 1994. The calcium feedback signal in the phototransduction cascade of vertebrate rods. *Neuron.* 13:849–861.
- Grunwald, M.E., W.P. Yu, H.H. Yu, and K.W. Yau. 1998. Identification of a domain on the beta-subunit of the rod cGMP-gated cation channel that mediates inhibition by calcium-calmodulin. *J. Biol. Chem.* 273:9148–9157.
- Gutfreund, H. 1995. Kinetics for the life sciences. Cambridge University Press. Cambridge, UK.
- Hackos, D.H., and J.I. Korenbrot. 1997. Calcium modulation of ligand affinity in the cGMP-gated ion channels of cone photoreceptors. *J. Gen. Physiol.* 110:515–528.
- Haynes, L.W., and S.C. Stotz. 1997. Modulation of rod, but not cone, cGMP-gated photoreceptor channel by calcium-calmodulin. *Vis. Neurosci.* 14:233–239.
- Haynes, L.W., and K.W. Yau. 1990. Single channel measurement from the cGMP-activated conductance of catfish retinal cones. *J. Physiol.* 429:451–481.
- Hestrin, S., and J.I. Korenbrot. 1987. Effects of cyclic GMP on the kinetics of the photocurrent in rods and in detached rod outer segments. *J. Gen. Physiol.* 90:527–551.
- Hsu, Y.T., and R.S. Molday. 1994. Interaction of calmodulin with the cyclic GMP-gated channel of rod photoreceptor cells. Modulation of activity, affinity purification, and localization. *J. Biol. Chem.* 269:29765–29770.
- Kawamura, S. 1993. Rhodopsin phosphorylation as a mechanism of cyclic GMP phosphodiesterase regulation by S-modulin. *Nature.* 362:855–857.
- Kawamura, S., O. Kuwata, M. Yamada, S. Matsuda, O. Hisatomi, and F. Tokunaga. 1996. Photoreceptor protein s26, a cone homologue of S-modulin in frog retina. *J. Biol. Chem.* 271:21359–21364.
- Kleene, S.J. 1999. Both external and internal calcium reduce the sensitivity of the olfactory cyclic-nucleotide-gated channel to cAMP. *J. Neurophysiol.* 81:2675–2682.
- Kleinschmidt, J., and J.E. Dowling. 1975. Intracellular recordings from gecko photoreceptors during light and dark adaptation. *J. Gen. Physiol.* 66:617–648.
- Koch, K.W., and L. Stryer. 1988. Highly cooperative feedback control of retinal rod guanylate cyclase by calcium ion. *Nature.* 334: 64–66.

- Korenbrodt, J.I., and D.L. Miller. 1989. Cytoplasmic free calcium concentration in dark-adapted retinal rod outer segments. *Vision Res.* 29:939–948.
- Kurahashi, T., and A. Menini. 1997. Mechanism of odorant adaptation in the olfactory receptor cell see comments. *Nature.* 385: 725–729.
- Koutalos, Y., K. Nakatani, and K.W. Yau. 1995. The cGMP-phosphodiesterase and its contribution to sensitivity regulation in retinal rods. *J. Gen. Physiol.* 106:891–921.
- Lagnado, L., and D.A. Baylor. 1994. Calcium controls light-triggered formation of catalytically active rhodopsin. *Nature.* 367: 273–277.
- Lagnado, L., L. Cervetto, and P.A. McNaughton. 1992. Calcium homeostasis in the outer segments of retinal rods from the tiger salamander. *J. Physiol.* 455:111–142.
- Liu, M., T.Y. Chen, B. Ahamed, J. Li, and K.W. Yau. 1994. Calcium-calmodulin modulation of the olfactory cyclic nucleotide-gated cation channel. *Science.* 266:1348–1354.
- Lolley, R.N., and E. Racsz. 1982. Calcium modulation of cyclic GMP synthesis in rat visual cells. *Vision Res.* 22:1481–1486.
- Malchow, R.P., and S. Yazulla. 1986. Separation and light adaptation of rod and cone signals in the retina of the goldfish. *Vision Res.* 26:1655–1666.
- Maricq, A.V., and J.I. Korenbrot. 1990. Potassium currents in the inner segment of single retinal cone photoreceptors. *J. Neurophysiol.* 64:1929–1940.
- Martell, A.E., and R.M. Smith. 1974. Critical Stability Constants, Plenum Publishing Corp., New York, NY.
- Matthews, H.R. 1997. Actions of  $Ca^{2+}$  on an early stage in phototransduction revealed by the dynamic fall in  $Ca^{2+}$  concentration during the bright flash response. *J. Gen. Physiol.* 109:141–146.
- McCarthy, S.T., J.P. Younger, and W.G. Owen. 1994. Free calcium concentrations in bullfrog rods determined in the presence of multiple forms of Fura-2. *Biophys. J.* 67:2076–2089.
- Miller, D.L., and J.I. Korenbrot. 1987. Kinetics of light-dependent Ca fluxes across the plasma membrane of rod outer segments. A dynamic model of the regulation of the cytoplasmic Ca concentration. *J. Gen. Physiol.* 90:397–425.
- Miller, J.L., and J.I. Korenbrot. 1993. In retinal cones, membrane depolarization in darkness activates the cGMP-dependent conductance. A model of Ca homeostasis and the regulation of guanylate cyclase. *J. Gen. Physiol.* 101:933–960.
- Miller, J.L., and J.I. Korenbrot. 1994. Differences in calcium homeostasis between retinal rod and cone photoreceptors revealed by the effects of voltage on the cGMP-gated conductance in intact cells. *J. Gen. Physiol.* 104:909–940.
- Molokanova, E., F. Maddox, C.W. Luetje, and R.H. Kramer. 1999. Activity-dependent modulation of rod photoreceptor cyclic nucleotide-gated channels mediated by phosphorylation of a specific tyrosine residue. *J. Neurosci.* 19:4786–4795.
- Molokanova, E., B. Trivedi, A. Savchenko, and R.H. Kramer. 1997. Modulation of rod photoreceptor cyclic nucleotide-gated channels by tyrosine phosphorylation. *J. Neurosci.* 17:9068–9076.
- Murnick, J.G., and T.D. Lamb. 1996. Kinetics of desensitization induced by saturating flashes in toad and salamander rods. *J. Physiol.* 495:1–13.
- Nakatani, K., Y. Koutalos, and K.-W. Yau. 1995.  $Ca^{2+}$  modulation of the cGMP-gated channel of bullfrog retinal rod photoreceptor. *J. Physiol.* 484:69–76.
- Nikonov, S., N. Engheta, and E.N. Pugh, Jr. 1998. Kinetics of recovery of the dark-adapted salamander rod photoresponse. *J. Gen. Physiol.* 111:7–37.
- Normann, R.A., and I. Perlman. 1979. The effects of background illumination on the photoresponses of red and green cones. *J. Physiol.* 286:491–507.
- Normann, R.A., and F.S. Werblin. 1974. Control of retinal sensitivity. I. Light and dark adaptation of vertebrate rods and cones. *J. Gen. Physiol.* 63:37–61.
- Palczewski, K., I. Subbaraya, W.A. Gorczyca, B.S. Helekar, C.C. Ruiz, H. Ohguro, J. Huang, X. Zhao, J.W. Crabb, and R.S. Johnson. 1994. Molecular cloning and characterization of retinal photoreceptor guanylyl cyclase-activating protein. *Neuron.* 13:395–404.
- Pepe, I.M., A. Boero, L. Vergani, I. Panfoli, and C. Cugnoli. 1986. Effect of light and calcium on cyclic GMP synthesis in rod outer segments of toad retina. *Biochim. Biophys. Acta.* 889:271–276.
- Perlman, I., and R.A. Normann. 1998. Light adaptation and sensitivity controlling mechanisms in vertebrate photoreceptors. *Prog. Retin. Eye Res.* 17:523–563.
- Picones, A., and J.I. Korenbrot. 1992. Permeation and interaction of monovalent cations with the cGMP-gated channel of cone photoreceptors. *J. Gen. Physiol.* 100:647–673.
- Pugh, E.N., and T.D. Lamb. 1990. Cyclic GMP and calcium: the internal messengers of excitation and adaptation in vertebrate photoreceptors. *Vis. Res.* 12:1923–1948.
- Rebrik, T.I., and J.I. Korenbrot. 1998. In intact cone photoreceptors, a  $Ca^{2+}$ -dependent, diffusible factor modulates the cGMP-gated ion channels differently than in rods. *J. Gen. Physiol.* 112: 537–548.
- Rispoli, G., W.A. Sather, and P.B. Detwiler. 1993. Visual transduction in dialysed detached rod outer segments from lizard retina. *J. Physiol.* 465:513–537.
- Ruiz, M., R.L. Brown, Y. He, T.L. Haley, and J.W. Karpen. 1999. The single-channel dose–response relation is consistently steep for rod cyclic nucleotide-gated channels: implications for the interpretation of macroscopic dose–response relations. *Biochemistry.* 38:10642–10648.
- Sagoo, M.S., and L. Lagnado. 1996. The action of cytoplasmic calcium on the cGMP-activated channel in salamander rod photoreceptors. *J. Physiol.* 497:309–319.
- Sagoo, M.S., and L. Lagnado. 1997. G-protein deactivation is rate-limiting for shut-off of the phototransduction cascade. *Nature.* 389:392–395.
- Sampath, A.P., H.R. Matthews, M.C. Cornwall, J. Bandarchi, and G.L. Fain. 1999. Light-dependent changes in outer segment free- $Ca^{2+}$  concentration in salamander cone photoreceptors. *J. Gen. Physiol.* 113:267–277.
- Watanabe, S., and J. Shen. 1997. Two opposite effects of ATP on the apparent sensitivity of the cGMP-gated channel of the carp retinal cone. *Vis. Neurosci.* 14:609–615.
- Weitz, D., M. Zoche, F. Muller, M. Beyerermann, H.G. Korschen, U.B. Kaupp, and K.W. Koch. 1998. Calmodulin controls the rod photoreceptor CNG channel through an unconventional binding site in the N-terminus of the beta-subunit. *EMBO (Eur. Mol. Biol. Organ.) J.* 17:2273–2284.
- Williams, D.A., and F.S. Fay. 1990. Intracellular calibration of the fluorescent calcium indicator Fura-2. *Cell Calc.* 11:75–83.
- Yau, K.W., and K. Nakatani. 1985. Light-induced reduction of cytoplasmic free calcium in retinal rod outer segments. *Nature.* 313: 579.
- Zimmerman, A.L., G. Yamanaka, F. Eckstein, D.A. Baylor, and L. Stryer. 1985. Interaction of hydrolysis-resistant analogs of cyclic GMP with the phosphodiesterase and light-sensitive channel of retinal rod outer segments. *Proc. Natl. Acad. Sci. USA.* 82:8813–8817.